

The Effect of Rare Earth (RE) Metal Doping of ZnO, On Magnetic and Optical Properties of ZnO Crystals Structure

Gizachew Diga Milki^{1,*}

Abstract

The magnetic and optical properties of magnetic semiconductors relies on the crystal structure, type and amount of dopant ions, and particle size. Then, the effect of rare earth metal (Dy, Eu, and La) doping on crystal structures, magnetic properties and optical properties are seen. It is revealed that the optical band gap of ZnO decrease down from 3.37eV up on doping with RE metals. Then, the Hamiltonian of the system is determined by using the Heisenberg's and Greens theorem. The exchange integral is determined by 3D Heisenberg model while electronic states are calculated by the Green's theorem. The expected magnetism is due to defect states, quantum size effect and double exchange mechanism. For the ferromagnetic states, the exchange integral is positive while it is negative for the antiferromagnetic states. Retarded Green's theorem revealed that both Magnetic and optical properties of RE doped ZnO are interdependent phenomenon. The combined effect of magnetic and optical properties of RE: ZnO exhibit can be tailored for biomedical and bioelectronics' applications. Furthermore, the incorporation of rare earth (RE) ions such as Dy, Eu, and La into the ZnO lattice introduces localized magnetic moments that interact with the charge carriers of the host semiconductor, leading to enhanced spin polarization and modified electronic transitions. These dopant ions create defect sites, oxygen vacancies, and lattice distortions, which play a crucial role in tuning the magnetic and optical responses of the material. The reduction in band gap energy upon doping can be attributed to the formation of intermediate energy levels within the forbidden band, facilitating visible light absorption and improving photocatalytic efficiency. The interaction between the 4f electrons of RE ions and the 3d electrons of Zn²⁺ ions enhances the ferromagnetic coupling through exchange interactions.

Keywords: Exchange integral, double exchange, ferromagnetism, magnetic semiconductor, spin interaction, quantum size effect

INTRODUCTION

Advancement in science and technology has been coming vital in the improvement in chemical industries, medicine and electronics. Particularly, every growing demand of Photocatalytic process and biomedicine is major area where such advancement is greatly anticipated. To achieve this requirement

*Author for Correspondence

Gizachew Diga Milki
E-mail: phygidg@gmail.com

¹Assistant Professor, Department of Physics, Jimma University, Ethiopia

Received Date: September 20, 2025

Accepted Date: October 10, 2025

Published Date: December 18, 2025

Citation: Gizachew Diga Milki. The Effect of Rare Earth (RE) Metal Doping of ZnO, on Magnetic and Optical Properties of ZnO Crystal's Structure. International Journal of Crystalline Materials. 2025; 2(2): 28–40p.

emphasis is given to the engineering of diluted magnetic semiconductors. Diluted magnetic semiconductors (DMS) are an interesting focus of solid-state physics, spintronics, optoelectronics, material science, nanotechnology, and biomedical devices. Among the DMS, RE metal doped ZnO is the best candidate. It has drawn greater attentions due to its measurable magnetic and optical properties. ZnO is direct wide band gap semiconductors. However, RE doping can shrink its band gap energy down to the narrow band gap semiconductor. RE (Dy, Eu, and La) can be

synthesized by various methods. As the research of Huang et al. 2014 [1] indicates, Eu^{3+} and D^{3+} can be synthesized by simple co-precipitation method. Moreover, Khataee, A., et al. 2020 [2], demonstrated that Eu doped ZnO nanocrystals can be synthesized by sonochemical method and characterized by XRD & XPS. As calculated by the Scherer's formula, the averages particles size of RE metal doped is shown in the Table 1.

The research of Smith, A. M, and Nie, S., 2010 [10] indicate that the quantum confinement effect in semiconductor nanoparticles widen their band gap and enable an efficient light emitter. This confinement determines the electrical, piezoelectric, ferroelectric and magnetic properties of nanostructure. As Suyitno et al. 2017 [11] detected, the efficiency of ZnO based piezoelectric nanogenerator can be modified by doping with TM and RE metals.

As Röder, R., 2019 [12] revealed, rare earth elements occupy Zn^{2+} sites in ZnO. Thus, ionization states of Zn^{2+} can effectively substituted with RE^{3+} ion. By increasing the concentration of RE ions (Dy, Eu, & La), Fermi level can moves into the conduction band of ZnO films. This mechanism can modify the electrical properties of ZnO.

The magnetic moments of rare earth (RE) metals of 4f electronic configuration are greater than 3d transition metals. Consequently, they exhibit better electrical, magnetic and optical properties upon doping with ZnO. As Tan C., et al. 2015 [13] observed, Ce, Eu, Gd, and Dy doped ZnO monolayer exhibit large magnetic moment. This magnetic moment is attributed to the role of RE atoms and slightly from nearest- neighbor O - atoms. RE metal doped ZnO has several applications including Photocatalytic activity, solar panels, LED, and photoconductors. Goel s., et al. 2017 [14] also notified that La doped ZnO nanocrystals is extensively used in photovoltaic materials for dye sensitized solar cells.

RE doped ZnO nanoparticles is used in print inks, artificial fertilizers, figure print analysis, biosensors, detecting enzymes and other bio molecules. As Sood, S. 2025 [15] noted, RE doping can considerably enhances ZnO's performance in electronic devices, like UV photo detectors, LEDs, and gas sensors. As Krishnaswamy, S. et al. 2025 [16] verified, Dy doped ZnO has unique optical and magnetic properties which make it valuable in optoelectronics and spintronics.

Moreover, ZnO doped with RE metal has a potential application in nanomedicine. Furthermore, the biomedical application of RE doped ZnO is presented in detail by the end of this manuscript.

CRYSTAL STRUCTURE OF RE: ZNO

ZnO is a binary semiconductor which major candidate in nanomedicine, optoelectronics, and photocatalytic process due to its biocompatibility, stability, and wide band gap. It has hexagonal wurtzite crystal structure where with lattice constant $a = 0.33\text{nm}$ and $c = 0.52\text{nm}$. Its periodic structures are nanowires, nanosheets, Moire patterns, and periodic pattern of quatum dots.

Table 1. Show the band gap of selected Dy, Eu, and La doped ZnO.

DMS	Lattice constant	Crystal size	Energy band gap	Reference
Dy: ZnO	3.319 Å	25.5 nm	3.26 eV- 3.34 eV	Zhang C. Y., et al 2010 [3]
			2.93 eV- 3.22 eV	Fidha, G. E. et al. 2021 [4]
Eu: ZnO	3.324 Å	34.87 μm 19nm-22nm (FTIR result)	3.13 eV	Gurbani, N. et al. 2023 [5]
			3.05 eV to 2.89	Kumar, P. et al. 2025 [6]
La: ZnO	c/a = 1.612	35.4 nm -59.3 nm	3.37eV to 2.6 eV	Pascariu, P. 2025 [7]
				Raina, I., et al. 2025 [8]
				Mansy, S., et al. 2023 [9]

Average band gap energy of ZnO: 3.37eV and Ionization energy ($E_a = 60\text{ eV}$)

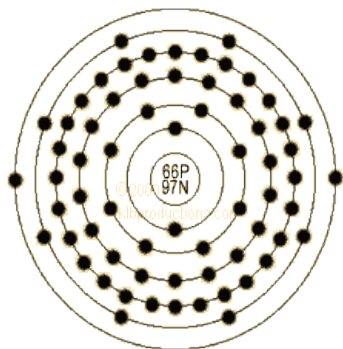


Figure 1. Electronic structure and configuration of Dy.

Electronic configuration: [Xe] 4f¹⁰6s²
Electronegativity: 1.22 eV
Electron work function: -
Ionization Potentials:
1st: 5.94 eV
2nd: 11.67
3rd: 22.802 eV.
Valence electron Potential: 47.7eV.

Kenneth Barbalace. 1995-2025 [19]

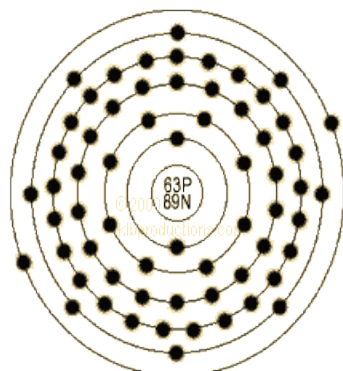


Figure 2. Electronic structure and configuration of Eu.

Electronic configuration: [Xe] 4f⁷6s²
Electro negativity: 1.2 eV
Electron work function: 2.5 eV
Ionization Potentials:
1st: 5.567 eV
2nd: 11.124
3rd: 24.926 eV.
Valence electron Potential: 45.6 eV.

Kenneth Barbalace. 1995-2025 [19]

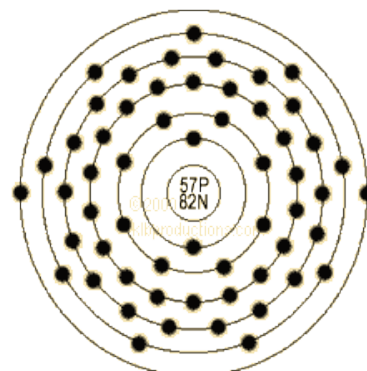


Figure 3. Electronic structure and configuration of La.

Electronic configuration: 5p¹6s²
Electro negativity: 1.1 eV
Electron work function: 3.5 eV
Ionization Potentials:
1st: 5.58 eV
2nd: 11.059 eV
3rd: 19.174 eV.
Valence electron Potential: 40.71 eV.

Kenneth Barbalace. 1995-2025 [19]

ZnO nanoparticles are semiconductor nanostructures with sizes 1- 20nm. In order to modify their physical, chemical and biological properties, they are often doped with either transition metals or rare earth metal ions. In this manuscript, RE (Dy, Eu, and La) doped ZnO particles are emphasized due to their leading applications in biomedicine, photocatalytic process, optoelectronics, and spintronics. Although, RE doped ZnO have the same crystal structure to bulk nanoparticles, they have unique magnetic and optical properties.

TM and RE metal-doped ZnO exists in three-lattice structure, namely wurtzite, Zinc blend and rock salt. Jayachandriah C., et al. 2014 [17] revealed, the ionic radius of Dy³⁺ is 0.91Å that is greater than Zn²⁺ of atomic radius 0.74 Å. Therefore, doping Dy in to ZnO crystal reduces the crystal size of Dy doped ZnO. Besides, Yan, B, Chen, X, Wu, J. H., 2007 [18], shown that Dy doped ZnO Nanofilms synthesized by rf Magnetron sputtering on Si & glass substrate showed hexagonal wurtzite structure Figure 1-3.

To sum up, doping ZnO nanoparticles with rare earth metal (RE) does not change the hexagonal wurtzite structure and shape. However, it may changes the lattice parameters leading to change in size.

This is due to the caused by changes in amount of RE ion concentration and atomic radii. The substitution of Dy³⁺ into ZnO matrix, reduce the Exciton recombination. This makes Dy: ZnO for Photocatalytic applications. This concept provides a high probability to explore the origin of RTFM in RE doped ZnO.

Defect And Impurity States

In diluted magnetic semiconductors defect are formed due to the high density of mismatch dislocations. The MSGF method is applied to describe the behavior of crystals containing lattice defects such as vacancies, interstitials, or foreign atoms. Studying these lattice defects is important due to their

role in materials technology. Introduction of defects into the crystal lattice of RE doped ZnO displaces the host atoms from their original position. Doping of ZnO nanocrystals with al selected elements (Dy, Eu, and La) tends to increase increase the defect states and density. These defects are potential in controlling the magnetic and optical properties of ZnO nanoparticles. Xin, M. 2018 [20] Eu-doped ZnO, common native defects like oxygen vacancies (V_o) and zinc interstitials (Zn_i) are present, and the incorporation of Eu can create new defects determined by super cell approach. The total number of defects is estimated from the exponentially decaying function

$$N = N_o e^{\frac{-E_a}{K_B T}} \quad 1$$

Where, N_o is the number of point defects at room temperature, E_a is the ionization energy, T is absolute temperature, and K_B is Boltzmann constant.

Introducing Eu dopant into host ZnO crystal cannot change the crystal structure of ZnO. However, it increase the number of defect related energy level. Eu shrinks the energy band gap which can alter its electrical and optical of ZnO. As Divya, N., & Pradyumnan, P. 2015 [21], revealed that Eu^{3+} doped ZnO at room temperature show enhanced visible light emission due to induced defects. As explained by Dakhel A. A., and Hilo M, E. 2010 [22], doping of ZnO with Gd at 3.5% creates large number of oxygen vacancies. These vacancies are responsible for the observed ferromagnetism in $Zn_{1-x}Gd_xO$. Moreover, doping of ZnO nanocrystals with RE (Dy, Eu, and La) creates shear strain and defects. This phenomenon tends to add the number of dislocations and surface imperfections.

Theoretical Approach: Multiscale Green's Theorem

Multiscale Green's function (MSGF) is a generalization of the classical Green's function (GF) designed for solving mathematical equations. It is an independent branch of science. As Wei S. H., 2004 [23] revealed, in computational physics and tight-binding lattices, recursive techniques is recognized for nanomaterials modeling. Moreover, Fasoline A. 2011 [24] verified that 2D nanomaterials including Graphene can be modeled by the same approach. Now a day's MSGF serves as more relevant for modeling of nanomaterials. These Materials are in the order of few nanometers.

The Green Functions (GF) is not limited to nanomaterials modeling. It can be used in modeling many physical processes in such as phonons, electronic band structure, density of states, and magnetic spin states. Nanomaterials are of atomistic dimensions and need to be modeled at the length scales of nanometers. Dy, Eu and La doped ZnO nanoparticles can also be modeled by MSGF. It can also describe the behavior of crystals containing lattice defects such as vacancies, interstitials, or foreign atoms. Studying these lattice defects is important due to their role in materials technology. Introduction of defects into the crystal lattice of RE doped ZnO displaces the host atoms from their original position.

The Hamiltonian of the Impurity State

In a system with multiple electrons per atom or in rare-earth materials, the spin-orbit coupling is replaced by spins total angular momentum.

$$H = H_o - \mu N + H_{exc} \quad 2$$

Where N is the total number particles, H_o is the unperturbed Hamiltonian H_{exc} is the Hamiltonian for spin exchange, and μ is the chemical potential of electrons.

Hence, for the magnetic interaction, we begin from the exchange Hamiltonian term. Whence,

$$H_{exc} = 2J \sum_{ij} S_i S_j \quad 3$$

The retarded Green function for two Fermions operators $S_i(t)$ and $S_j(t')$ in the Heisenberg representation can be defined as

$$\langle\langle S_i(t') / S_j(t') \rangle\rangle = -i\theta(t - t') \{S_i(t), S_j(t')\} \quad 4$$

Where $[S_i, S_j] = S_i S_j + S_j S_i$; is the Fermions anti commutation relation, $i\theta$ is the step function, and $\langle \dots \rangle$ means the ensemble average with the partition function, Z . Since $\langle \langle S_i(t') / S_j(t') \rangle \rangle$ is a function of $(t - t')$, it is convenient to define the Fourier transform

$$\langle \langle S_i / S_j \rangle \rangle = \int_{-\infty}^{+\infty} d(t - t') \langle \langle S_i(t') / S_j(t') \rangle \rangle e^{i\omega(t-t')} \quad 5$$

It can be shown that the retarded Green function in frequency space satisfies the equation of motion;

$$\omega \langle \langle S_i / S_j \rangle \rangle_m = \langle \{S_i, S_j\} \rangle \langle \langle [S_i, E] / S_j \rangle \rangle_m \langle \langle [S_i, E] / S_j \rangle \rangle_m \quad 6$$

Where again $\{S_i, S_j\}$ is the anticommutator of operators S_i & S_j , and $[S_i, E]$ is the commutator of the operators S_j and E . The ensemble average $\langle S_i(t') / S_j(t') \rangle$ can be calculated by

$$\langle \langle S_i(t') / S_j(t') \rangle \rangle = \int_{-\infty}^{+\infty} \frac{d\omega e^{-i\omega(t-t')}}{2\pi e^{i\omega+1}} [\langle \langle S_i / S_j \rangle \rangle_m - \langle \langle S_i / S_j \rangle \rangle_m] \quad 7$$

Where

$$\int_{-\infty}^{+\infty} \frac{d\omega e^{-i\omega(t-t')}}{2\pi e^{i\omega+1}} = 1 \quad 8$$

And $2 = \frac{e^{-i\omega(t-t')}}{2\pi e^{i\omega+1}}$, is a spectral function,

Where, in the equation 3.7

$$\langle S_i / S_j \rangle_{0,m} = \frac{2m}{\omega - \omega_0} \quad 9$$

Where, $m = \langle S_i^z \rangle$ is the averaged magnetization and $\langle S_i / S_j \rangle = \delta_{ij} = \begin{matrix} 0 & \Leftrightarrow & i \neq j \\ 1 & \Leftrightarrow & i = j \end{matrix}$. In this study, we consider only a 3D square lattice system in order to reduce complexity.

$$\langle \langle S_i^z S_j^+ / e^{as j^z} S_j^- \rangle \rangle \geq \langle S_i^z \rangle \langle \langle S_j^+ / e^{as j^z} S_j^- \rangle \rangle \quad 10$$

We can decouple the equation 3.9 in to the following form

$$\langle \langle S_i^z S_j^+ + S_i^- S_j^+ / e^{as j^z} S_j^- \rangle \rangle = 2J \langle S_i^z \rangle \langle \langle S_j^+ / e^{as j^z} S_j^- \rangle \rangle \quad 11$$

Implying that

$$J_s = 1 - \frac{1}{2S^2} [S(S+1) - 2(S_i^z)^2] \quad 12$$

Where

$$(S_i^z)^2 = S(S+) - S_i^- S_j^+, \setminus$$

Taking $S = 2$, for D_y , the exchange integral is expressed as;

$$J = 1 - 0.125 [\langle (S_i^z)^2 + S_i^- S_j^+ \rangle] \quad 13$$

J_s is a dimension less constant which describes ferromagnetic order. It approaches zero in the thermodynamic limit above T_c and unity below T_c . From finite size scaling theory, it is revealed that this constant is size independent at the critical temperature. Below T_c , J , increases as system size increases, while J decreases as system size increases above T_c .

From first principle calculations, Shi Y. et al. 2010 [25] determined that the coupling between Gd ions in ZnO is ferromagnetic and appropriate concentration; electrons can enhance the ferromagnetic coupling between them. However, for Nd ions, the holes of appropriate concentration can enhance the ferromagnetic coupling between them.

In the ZnO: Dy system, the s- f coupling is much larger than the f - f and f-p couplings, electron-mediated ferromagnetism in ZnO: Dy system. Dysprosium has atomic number 66, and its ground state is listed as 5I_8 . As Griffith, D. 2005 [26] states the spin and angular magnetic moments of this state with $S = 2$, $L = 6$ and $J = L + S = 8$.

The Land g - factor is given by

$$g = \frac{3}{2} + \frac{J(J+1)+S(s+1)-L(l+1)}{2J(J+1)} = 2.00 \quad 14$$

T.Thangeeswari and his coworkers [27] invented room temperature ferromagnetism in Dy: ZnO and Yb: ZnO nanoparticles. The origin of ferromagnetism estimated from the magnetic exchange interaction between oxygen vacancy and Dy^{3+} , Yb^{3+} ions forming bound magnetic Polaron. The effective number of Bohr Magnetron for the Dy^{3+} is 10.6.

$$\langle m \rangle = \frac{g^2 \mu_B^2 J(J+1)}{3 K_B T} \vec{B} \quad 15$$

Where $\langle m \rangle$ average of reduced magnetization, J , is the exchange integral, T -is temperature, and \vec{B} is magnetic field. As Junaid M et al. 2021 [28] Spectroscopic and quantum sizing technologies can be employed to determine the crystal size. As revealed, Powder X-rays can help to determine the crystal size and Phases of ZnO.

RESULTS AND DISCUSSION

Many researchers and experimenters have been studied the physical properties of such ZnO and RE separately. In this discussion, the parameters ascribing the phenomenon of magnetism and optical property are discussed. As the discussion, revealed, the magnetic and optical characteristics of the host and RE doped ZnO nanostructures have shown interdependence.

Not only induced defects but also native defects will contribute for the ferromagnetic property. However, further heating the sample will reduce the saturation magnetizations and quenching of wavelength, which reinforce paramagnetic. In this section, the effect of RE doping on both magnetic optical properties is seen.

Effect Of RE Doping

Magnetic properties

RE doping has been found a useful means to engineer electronic band structure, crystal structure, and lattice parameter. It is a means to deliberately introducing defect states responsible for color emissions and magnetic properties. In this section, the effect of RE doping, temperatures and magnetic field in controlling the magnetic property of Dy doped ZnO is discussed in comparison with transition metal doped ZnO. The poles of the function in equation 3 are obtained at, $\omega = \omega_o$.

The magnetic properties of RE doped ZnO are closely related with defects. In case of RE(Dy, Eu, & La) doped ZnO, the origin of magnetism is associated with oxygen vacancies. Native defects such as Zn interstitial and an Oxygen vacancy creates local magnetic moments. Besides, La doping induces d_0 ferromagnetism although it lacks 4f-electron. Doping ZnO with La, generate ferroelectricity. Moreover, as Cong Li. Et al. 2018 [29] verified localized moments are coupled over long distances through the conduction electrons and create long-range magnetic order in ZnO doped La. As reported by J. S. Malhotra et al. 2018 [30], 2% Dy doped ZnO shows the blend of weak ferromagnetic and paramagnetic behavior. Dy doped ZnO and Yb: ZnO nanoparticles show ferromagnetic properties due to the rare earth dopant. As compared to TM such Mn, Co, Ni and Fe doped ZnO, RE doped ZnO exhibits weaker ferromagnetism.

The graph shows that the ferromagnetic magnetization as the frequency of the resonator increase. This is because as magnetization has inverse relations with temperature and thus with giant magneto resistance, the frequency increase above the natural frequency of the resonator. The phenomenon has the same feature as the electric potential which declines as the separation between electric charges increases Figure 4.

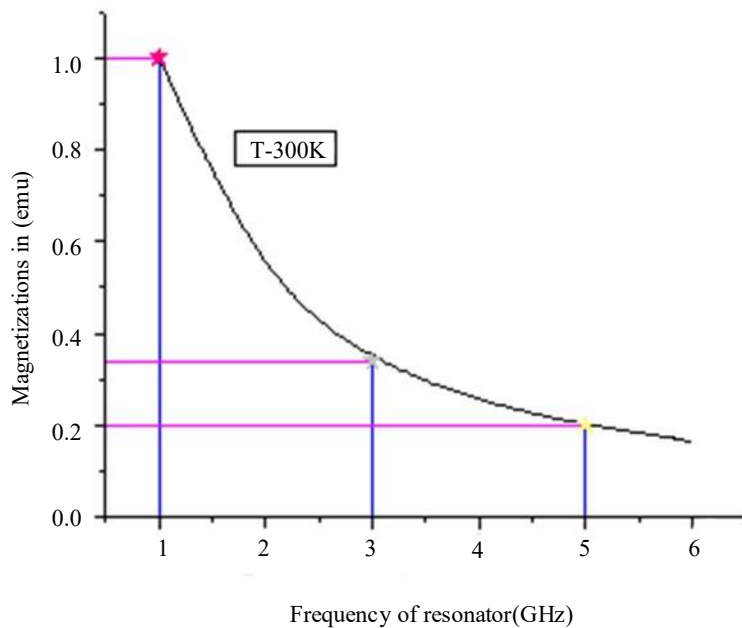


Figure 4. Magnetization against frequency of ferromagnetic resonator for dy doped ZnO.

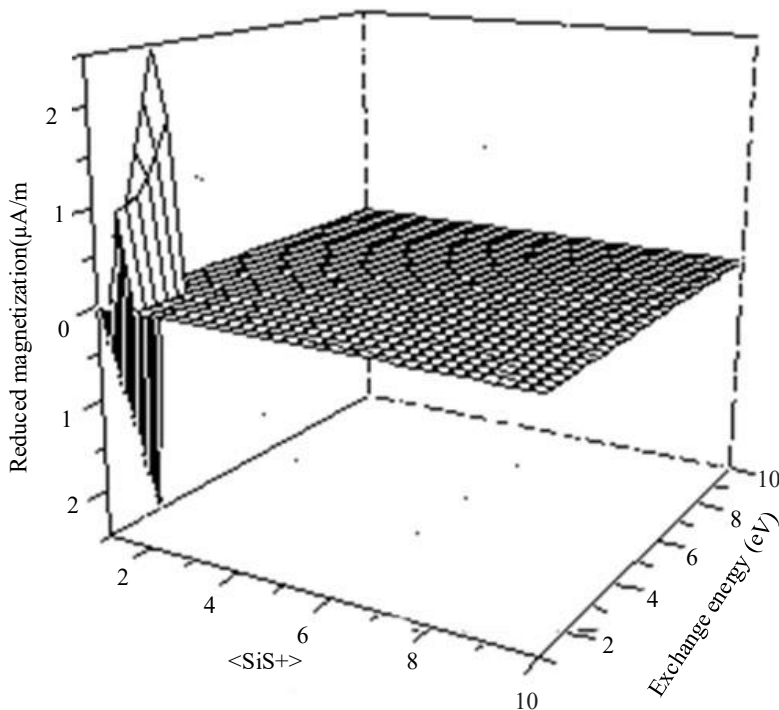


Figure 5. The relations among the exchange integral, and reduced magnetization; RE:ZnO.

As illustrated in the figures, the exchange energy varies with the spin mixing. The value of reduced magnetization oscillates between $-3\mu\text{A/m}$ to $3\mu\text{A/m}$. It is pass through the equilibrium point at a value equal to exchange integral, 1eV . However, it shows a sharp increase for a magnetization greater than $2.0\mu\text{A/m}$ to $3\mu\text{A/m}$. It also decrease in the fashion in the range, $-2.0\mu\text{A/m}$ to $-3\mu\text{A/m}$. However, in the range $-1\mu\text{A/m}$ to $0\mu\text{A/m}$ and or $0.0\mu\text{A/m}$ to $1\mu\text{A/m}$ it changes slowly. In general, figure 5 at constant exchange energy, the magnetic moment oscillates at finite frequency as any other electromagnetic waves do. Consequently, RE doped, ZnO exhibits weak magnetic moment unlike to metal ferromagnets.

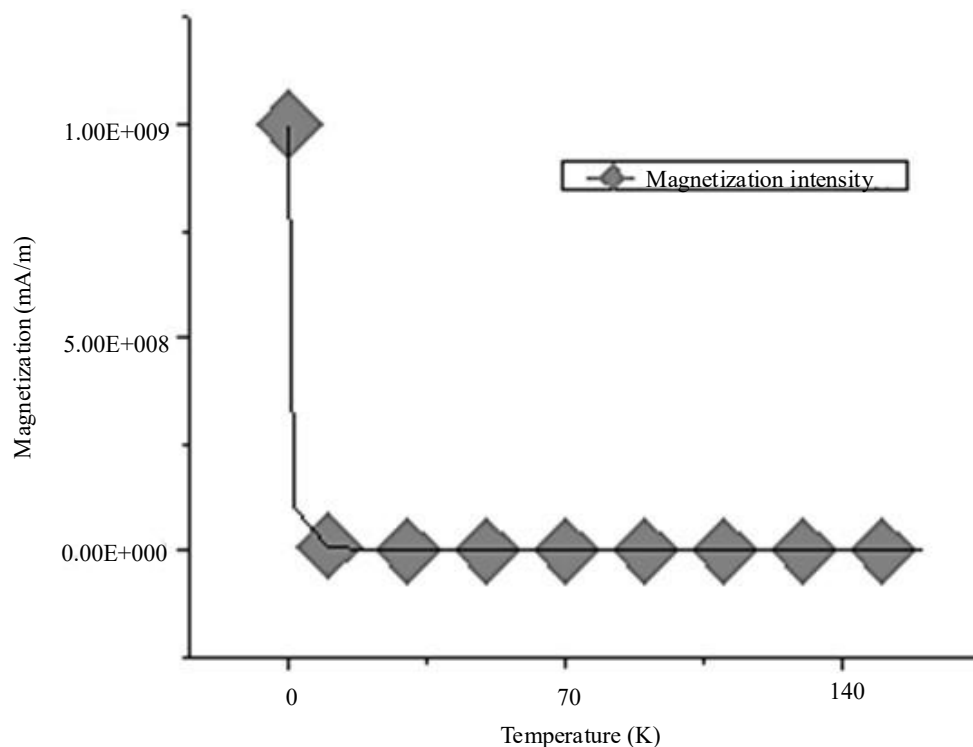


Figure 6. The change in magnetization with temperature.

As shown in the Figure 6, the magnetization decreases with temperature. The magnetization gets infinite at a temperature closer to the room temperature. In addition, defect and color centers. This result resembles with the experimental result, Yoon et al., 2012 [30] of Eu doped ZnO with varying Eu concentrations. This reveals that the ferromagnetic states are associated with defects (oxygen vacancy) and secondary phases. Moreover, Eu doped ZnO exhibit weak ferromagnetism associated with Eu^{3+} ions and bound magnetic Polaron. Unlike to transition metal doped ZnO, the magnetic moments of RE doped ZnO arises from the 4f incomplete sub shell.

Unlike to metal nanoparticles such as Ag, which shows surface Plasmon resonance, rare earth metal doped ZnO nanoparticles exhibits confinement of delocalized energy states. This confinement due to Dy^{3+} ion cluster around the oxygen anion leads to the weak FM order. The spin component of $\text{Zn}_{1-x}\text{Dy}_x\text{O}$ is isotropic, whereas the orbital component reflects the symmetry leading to anisotropic effects.

As CaO H. et al. 2014 [31] verified, in $3d^5$ ions such as Fe^{3+} or Mn^{2+} , doped ZnO, the Fe and Mn takes the substitutional Zn^{2+} . Hence, the donor electron is down spin and the effective coupling between two magnetic impurities falling within the same donor orbital is ferromagnetic. However, Tan C., 2014 [13] revealed that in Rare Earth (RE = Ce, Dy, Eu, Gd & La)-doped ZnO, unpaired spins are primarily located on the localized f-state of the ion. Particularly, Dy doped ZnO nanoparticles show the ferromagnetic properties due to the rare earth dopant. Similar fashion, Daksh and Agrawal Y. K. 2016 [32-33] verified a shift from diamagnetic to weak ferromagnetism for Nd doped ZnO. RE metals Ce, Eu, Gd, and Dy doped ZnO monolayer's exhibits magnetic properties due to spin polarization between the DOS of up and down spin channels near the Fermi level. ZnO: Eu to ZnO: Yb the near configuration fluctuates around zero between the ferromagnetic and the antiferromagnetic states.

Optical Properties

Most rare earth metal ion has high atomic radii. Consequently, doping ZnO with rare earth metal increases its optical band gaps by Burstein-Moss effect. Particularly, doping of ZnO with La decreases the energy band gap. Although, La doping doesn't typically change the hexagonal crystal structure of

ZnO, it can introduce lattice distortions and defects such as oxygen vacancies. These vacancies not only change the optical properties but also the magnetic properties of ZnO. This kind of doping can increase the transmission coefficient.

The defects are responsible for color emissions governed XRD diffraction (Bragg's law).

$$2d\sin\theta = n\lambda \quad 16$$

Where λ is the wavelength, θ is the diffraction angle, and d - is the spacing between parallel planes, n - is order of diffraction. Using the Fraunhofer diffraction, and Bragg diffraction condition, the intensity profile can be calculated.

$$I(\theta) = \frac{2\hbar c^2}{\pi^2 \lambda^4} (1 - \cos^2(\theta)) \quad 17$$

Unlike to Dy and La doping, Eu doping of ZnO introduces a sharp, line emissions around the wavelength, $\lambda = 615.8\text{nm}$. Hence, for the case of Eu doped ZnO as a prime example,

$$I(\theta) = 13.4 \times 10^6 \frac{w}{m^2} (1 - \cos^2(\theta)) \quad 18$$

$I(\theta)$ is intensity as a function of angular displacement. This is due to transition of Europium ion, Eu^{3+} at 4f-4f electronic configuration. Consequently, it leads to energy transfer between defect levels resulting in luminescence quenching.

As the Figure 7 illustrates, the intensity has shown a phase shift for every 90 degrees, periodically. This is due to the consequence of the crystalline nature of ZnO nanoparticles and RE doped ZnO. The calculation above is performed in the first and second Brillouin zone. The pattern of intensity as function of half width maxima is illustrated by Sugihartono et al. 2023 [34-35] in case of La doped ZnO. The Wavelength of La: ZnO is 613 nm which almost closer to the wavelength of Eu^{3+} doped ZnO. Thus, one can follow the same approach in order to investigate the change in intensity with angular displacement, θ .

These quenching not only influence the optical property but also impinges the magnetic properties of ZnO nanoparticles. According to J. M. D. Coey, 2010 [34] nanoparticles are long-wavelength spin waves, which cannot be excited because the particle size fixes a maximum possible wavelength, like Magnons.

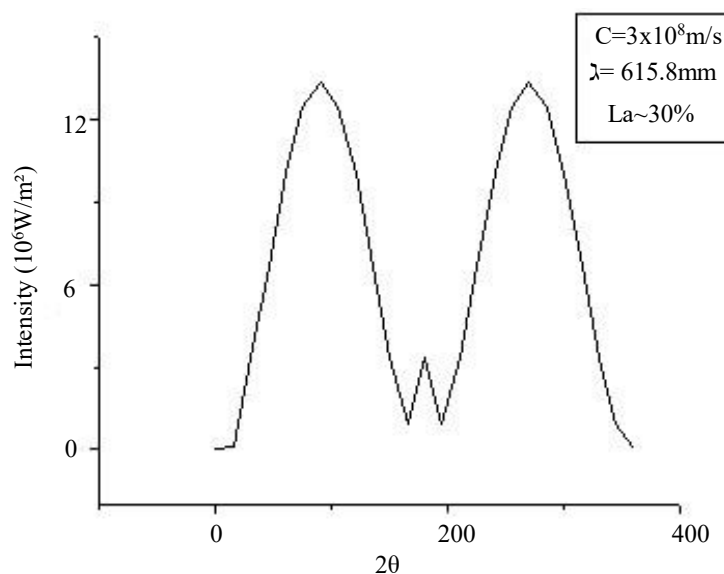


Figure 7. The nature of Intensity as with half width half maxima

RE metal doped ZnO in Action

Photonics and Photocatalytic activity

ZnO nanostructure has been emerged as a potential candidate in Photocatalytic activity. Their ability to absorb light at defined wavelength range enables it useful in optical and magnetic sensor. ZnO is an important material in photonic devices, and photo catalyst. RE doped ZnO nanocrystals are good candidate for flat solar panel display phosphors due to efficient emission in the visible range. Another important applications of magnetic nanoparticles include, bioprocessing, color imaging, and forming ferrofluid for magnetic fluid hyperthermia.

Dy has been regarded as an efficient dopant for ZnO nanoparticles to improve Photocatalytic activity. $Zn_{1-x}Dy_xO$ is outstanding nanomaterials for Photocatalytic application. As stated by Yang J et al. 2018 [36], Dy doping in the ZnO crystal lattice reduce electron hole recombination, which is precondition for Photocatalytic activity. As Wang Y. et al. 2016 [37] stressed, both the Mn^{2+} and N doping can induce large amounts of surface defects which exhibits a strong Photocatalytic activity. Dhiman, P., et al. 2023 [38] also demonstrated that Dy doped ZnO exhibits maximum degradation efficiency of 74.19% for removing tetracycline. Tripathy, N & Kim, D., 2018 [39] had revealed that the biosensing efficiency of ZnO nanostructures can be modified by Metal oxide.

As Song Z., et al. 2011 [40] Nonlinear optical microscopy provides means for high-contrast imaging of ZnO NPs lending in vitro and in vivo assessment of the nanoparticles uptake in skin, Dy doped ZnO is practically used as photo detector, particularly UV- detector. ZnO doped with Dy^{3+} is characterized by emitting white light. A research findings, Pangul C. N., et al. 2018 [41] shows that Dy^{3+} doped ZnO nanofibers possess denser emissions at visible light region. In general, RE doping of ZnO increase the hydroxide radical and fasten photo degradation process. Consequently, RE (Dy, Eu and La) doping of ZnO enhance its photo catalytic process by delaying Exciton recombination.

Biomedicine

ZnO nanoparticles can be resized and surface structured for high grade biomedical applications. ZnO nanoparticles can be designed as antibacterial, anticancer, and contrast agents. ZnO nanoparticles are sociable to human body cells and tissues due to their biocompatibility. These properties make ZnO nanoparticles for targeted nanocarriers, cell therapy, and Gene therapy and targeted drug delivery systems. As Mejía-Méndez, J. L. 2024 [42] published, RE metals such La doped ZnO nanoparticles have been reported to treatment of target neurological diseases. This research also revealed that machine learning approach can enhance therapeutic efficiency. ZnO nanoparticles are potentially used to treat leukemia and carcinoma cancer cell. It is also pharmaceutical products, and antibacterial.

It has novel applications in nanomachines that can act as biological mimetic, biomaterials for tissue engineering. As research of Bisht G., et al. 2016 [43] indicates, ZnO nanoparticles have a wide range of applications in cancer therapy, biosensing, drug/gene delivery. Muhammad Torequl Islam et al. 2017 [44] also demonstrates, Biosensors with photonic crystals are implemented for monitoring changes in proliferation and apoptosis of breast cancer cells. Moreover, as Carofiglio, M. et al. 2020 [45] demonstrated, RE metal doped ZnO is valuable in enhanced bio imaging, fluorescent imaging, antitumor and reactive oxidative species (ROS).

RE doped ZnO is also used in coding, genome editing, DNA bio labeling, and Gene sequencing due to its distinguished magnetic and optical properties. Dy, Eu, & La doped ZnO is widely used Bio imaging, visualizing DNA, and magnetic separations. It is also used biomedicine as targeted drug delivery, cancer therapy, cell labels and imaging, environmental health and safety. In practices, by optimizing and controlling the size, composition, crystal morphology, biophysical properties, RE doped ZnO can be leveraged for enhanced bioelectronics and biomedicine.

CONCLUSION

The magnetic properties of Dy doped ZnO is determined theoretically. Magnetic properties and exchange integral are determined by multicar greens functions. The calculated values, particularly, the

exchange integral and the Lande factor show that, Dy doped ZnO presents weak ferromagnetism. However, Dy has a high magnetic moment, $Zn_{1-x}Dy_xO$ exhibits weak ferromagnetism. The observed magnetism is due to the formation of defects, presence of Dy^{+2} and particle confinement. Compared to Mn doped ZnO, the observed ferromagnetism is weaker due to the fact p-d hybridization is stronger than d-f hybridization in Dy doped ZnO. In general, ZnO nanoparticles exhibit different magnetic and optical properties depending on the crystal structure, atomic size, amount of concentrations, size of interactions, and type of RE ions. By optimizing such varied physical properties RE doped ZnO can be tailored for enhanced bioelectronics, solar cells, photocatalytic activities, and biomedicine. Particularly, RE (Dy, Eu, and La) doping of ZnO improves the photocatalytic process such as degradation of dyes by delaying exciton recombination. Moreover, ZnO doped with Dy, Eu, and La increases the efficiency of biosensors for detecting pathogens, cancerous cells/tissues, and cardiovascular diseases. Consequently, doping ZnO with rare earth metal ions improves both magnetic and optical properties and enhances its biomedical and photocatalytic activity. In future work, RE (Dy, Eu, and La) doped ZnO guided by a magnetic field will be further studied for application in nanozymes and medical biotechnology.

REFERENCES

1. Huang et al. Optical properties of Eu, Dy co-doped ZnO Nanocrystals. *Optoelectronics Lett.* 2014, Vol. 10, 3(1), 0163.
2. Khataee, A., Karimi, A., Zarei, M., & Joo, S. W. (2020). Eu doped ZnO nanoparticles; Sonochemical synthesis, characterizations and photocatalytic applications. *Ultrasonic's sonochemistry*, 67, 102822. <https://doi.org/10.1016/j.ultsonch.2015.03.016> 2020
3. Zhang C. Y., et al. Structure and Optical properties of Dy doped ZnO film grown by RF Magnetic sputtering. *Advanced material research*. 2010, Vol. 97-101, page 11-14. <https://doi.org/10.4028/www.scientific.net/AMR.97-101.11>
4. Fidha, G. E. et al. Physical and Photocatalytic properties of Sprayed Dy doped ZnO thin films under light irradiations for degradation of methylene blue. *RSC Advances*. 2021, V.11 (40) 24917. <https://doi.org/10.1039/d1ra03967a>.
5. Gurbani, N., & Chouhan, N. (2023). P-N Hetero-junction systems Eu doped ZnO@Go for photocatalytic water splitting. *Global challenges*, 7(4), 22000106. <https://doi.org/10.1002/gch2.202200106>.
6. Kumar, P., Kumar, S., Kaur, H., Kumar, A., & Kumar, A. (2025). Optimizing Photocatalysis: Tuning europium concentration in zinc oxide nanoparticles for superior performance. *Physica B: Condensed Matter*, 697, 416699. <https://doi.org/10.1016/j.physb.2024.416699>
7. Pascariu, P., Nedelcu, O. T., Sandu, T., Romanitan, C., Brincoveanu, O., Pachiu, C., Manica, D., Manica, M., Popescu, A. G. M., Antohe, S., Ionescu, O. N., Sucheana, M. P., & Koudoumas, E. (2025). Lanthanum doping effects on microstructure and properties of nanostructured ZnO. *Materials Characterization*, 224, 114994. <https://doi.org/10.1016/j.matchar.2025.114994>
8. Raina, I., Kumar, P., Kumar, A., Singh, K., Somvanshi, A., Soni, R., & Kumar, D. (2025). Visible-light activated La-doped ZnO photocatalysts for enhanced degradation of crystal violet dye. *Ceramics International*. <https://doi.org/10.1016/j.ceramint.2025.09.158>
9. Mansy, S., et al. Computational and experimental study of wurtzite Phase ZnO nanoparticles. *Materials Today Communications*. 2023, V-35, 105688. <https://doi.org/10.1016/j.mtcomm.2023.105688>.
10. Smith, A. M., & Nie, S. (2010). Semiconductor Nanocrystals: Structure, Properties, and Band Gap Engineering. *Accounts of Chemical Research*, 43(2), 190. <https://doi.org/10.1021/ar9001069>
11. Suyitno et al., Simple Fabrication and Characterization of Piezoelectric nanogenerators from cobalt doped Zinc Oxide Nanofibers, *A.J. APP. Sci.* 2017, 14(7), 662-669.
12. Röder, R., Geburt, S., Zapf, M., Franke, D., Lorke, M., Frauenheim, T., & Ronning, C. (2019). Transition Metal and Rare Earth Element Doped Zinc Oxide Nanowires for Optoelectronics. *Physica Status Solidi (b)*, 256(4), 1800604. <https://doi.org/10.1002/pssb.201800604>
13. Tan et al. Electronic and magnetic properties of rare earth metals doped ZnO monolayer, *J. nanomaterials*. 2015, Vol. 2, 329-570

14. Goel, S et al. Experimental investigation on the structural, dielectric, ferroelectric and piezoelectric properties of La doped ZnO nanoparticles and their application in dye-sensitized solar cells, *Phys. E Low - dimens. System. Nanostructure.* 2017, 91, 72e8.
15. Sood, S., Kumar, P., Raina, I., Misra, M., Kaushal, S., Gaur, J., Kumar, S., & Singh, G. (2025). Enhancing Optoelectronic Performance through Rare Earth Doped ZnO: Insights and Applications. *Photonics*, 12(5), 454.
16. Krishnaswamy, S. et al. Investigation of the optical properties of Dy doped ZnO/PVA thin film: White light emission for LED application. *Results in Optics.* 2025, 18, 100786. <https://doi.org/10.1016/j.rio.2025.100786>
17. Zhang C., et al. Structural and Optical properties of Dy doped ZnO film Growth, by RF Magnetic sputter. *Advanced Material Research.* 2010, Vol. 97(101), Pp. 11-14. Doi. 10.4028/www.Scientific.Net/AMR. 97-101.11.
18. Jayachandraiah C., et al. Influence of Dy dopant on the structural and Photoluminescence of Dy doped ZnO nanoparticles. *Journal of alloys and Compounds.* 2014, V- 636, Doi: 10.1016/j. jallcom. 2014. 10. 067.
19. Kenneth Barbalace. Periodic Table of elements-“Rare Earth”. *Environmental chemistry. com*, 1995-2025, [https://Environmental chemistry. Com/Yogi/periodic /RE \(Dy, Eu,& La\).html](https://Environmental chemistry. Com/Yogi/periodic /RE (Dy, Eu,& La).html).
20. Xin, M. Effect of Eu doping on the structure, morphology and luminescence properties of ZnO submicron rod for white LED applications. *J Theore. Appl. Phys.* 2018, 12, 177–182. <https://doi.org/10.1007/s40094-018-0304-1>
21. Divya, N., & Pradyumnan, P. (2015). Solid state synthesis of erbium doped ZnO with excellent Photocatalytic activity and enhanced visible light emission. *Materials Science in Semiconductor Processing*, 41, 428-435. <https://doi.org/10.1016/j.mssp.2015.10.004>
22. Dakhel A, A. and Hilo M, E. Ferromagnetic nanocrystalline Gd doped ZnO powder synthesized by co precipitation. *J. Appl. Phys.* 2010, 107, 123905.
23. Wei S. H., *Computational materials science*, 2004, V. 30, 337
24. Fasoline A. Intrinsic ripples in graphene. *Nature Materials.* 2011, Vol. 6: 858–861
25. Shi Y., et al. Magnetic coupling properties of rare earth metals (Gd, Nd) doped ZnO: first - principles calculations, *J. Con. Matter Phys.* arxiv: 2010, 1005.1115. Vol. 1. Pp. 71.55.
26. Griffiths, David J. *Introduction to Quantum Mechanics.* 2005, 2nd ed.
27. T. Thangeeswari, G. Parthipan, and S. Gowtham, Impact of rare earth (Dy and Yb) ions doping on magnetic and optical properties of ZnO nanoparticles. 2019, 2105, 020003
28. Cong Li. Et al. Magnetic properties of La doped ZnO (0001)-Zn Polar surface with and without vacancies; First principle study. *Journal of superconductivity and Novel Magnetism.* 2018, 31 (9): 1-9, Doi. 10.1007/s10948-018-4564-4
29. J. S. Malhotra et al. investigations on structural, optical and magnetic properties of Fe and Dy co doped ZnO nanoparticles, *J. materials Science:* (2018) 29:3850–3855.
30. Junaid M et al. Band gap analysis of Zinc oxide for Potential bio glucose sensor. *Results in chemistry.* 2021, Vol. 3,100961.
31. Yoon H, Jun Hua Wu, Ji Hyun Min, Ji Sung Lee, Jae-Seon Ju et al. *J. Appl. Phys.* 2012, V. 111, 07 B-523
32. CaO H. et al. First principle study on electronic and magnetic properties of doped ZnO. *Journal of magnetism and magnetic materials.* 2014, 352(1):66-71. DOI: 10.1016/j. jmmm. 2023.10. 008.
33. Daksh and Yadendra Kumar Agrawal, Rare Earth-Doped Zinc Oxide nanostructures, *Rev. Nanosci & Nanotech*, 2016, Vol. 5, No. 1.
34. J. M. D. Coey (2010). *Magnetism and magnetic materials.* Cambridge University press. 7th ed. Pp. 264-300. www.combridge.org/9780521816144.
35. Sugihartono et al. Structural and Optical properties of La doped ZnO thin films at room temperature. *Processing and applications of ceramics.* 2023, 17(2), Pp 107-112. <https://doi.org/10.2298/PAC2302107S>.
36. Yang J. et al. Dy (III) Doped BiOCl Powder with Superior Highly visible – light- driven Photocatalytic Activity for Rhodamin B Photo degradation, *Nanomaterials.* 2018, 8, 697; doi:10.3390/nano8090697.

37. Wang Y., Jing Cheng, Suye Yu, Enric Juan Alcocer, Muhammad Shahid, Ziyuan Wang & Wei Pan, 2016, 6:32711
38. Dhiman, P et al. Rare Earth doped ZnO nanoparticles as a spintronics and Photo catalyst for degradation of Pollutants. *Molecule*. 2023, 28(6), 2838, <https://doi.org/10.3390/molecules28062838>.
39. Tripathy, N., & Kim, D. (2018). Metal oxide modified ZnO nanomaterials for biosensor applications. *Nano Convergence*, 5(1), 1-10. <https://doi.org/10.1186/s40580-018-0159-9>
40. Song Z, Timothy A. Kelf, Washington H. Sanchez, Michael S. Roberts, Jaro Rička, Martin Frenz, and Andrei V. Zvyagin, "Characterization of optical properties of ZnO nanoparticles for quantitative imaging of transdermal transport," *Biomed. Opt. Express* 2, 3321-3333 (2011).
41. Pangul CN, Anwane SW, Kondawar SB. Enhanced photoluminescence properties of electrospun Dy³⁺-doped ZnO nanofiber for white lighting devices. *Luminescence*. 2018 Sep;33(6):1087-1093. doi: 10.1002/bio.3513.
42. Mejia-Mendez, J. L., Navarro-López, D. E., Sanchez-Martinez, A., Ceballos-Sanchez, O., Garcia-Amezquita, L. E., Tiwari, N., Juarez-Moreno, K., Sanchez-Ante, G., & López-Mena, E. R. (2024). Lanthanide-Doped ZnO Nanoparticles: Unraveling Their Role in Cytotoxicity, Antioxidant Capacity, and Nanotoxicology. *Antioxidants*, 13(2), 213 <https://doi.org/10.3390/antiox13020213>
43. Bisht G., and Sagar Rayamajhi; ZnO Nanoparticles: A promising anticancer Agent, *Nano biomedicine*, 2016, 3:9 | Doi: 10.5772/63437.
44. Muhammad Torequl Islam, and Mohammad Ashab Uddin, *Biosensors, the Emerging Tools in the identification and Detection of Cancer Markers*, 2017, V. 5, ISSN, 2474-7602.
45. Carofiglio, M., Barui, S., Cauda, V., & Laurenti, M. (2020). Doped Zinc Oxide Nanoparticles: Synthesis, Characterization and Potential Use in Nanomedicine. *Applied Sciences (Basel, Switzerland)*, 10(15), 5194. <https://doi.org/10.3390/app10155194>